Article

Impact of Gap-Graded Soil Geometrical Characteristics on Soil Response to Suffusion

Chen Dong and Mahdi M. Disfani *

Department of Infrastructure Engineering, The University of Melbourne, Melbourne 3010, Australia;
cdong2@student.unimelb.edu.au
* Correspondence: mmiri@unimelb.edu.au

Abstract: The phenomenon of fine particle migration through the voids of the granule skeleton under the seepage force is called suffusion. Relative density, original fine particle content, and gap ratio are thought to play vital roles in the suffusion process. This paper investigates the effect of geometrical characteristics (i.e., original fine particle content, gap ratio, and relative density) on soil structure and mechanical performance (i.e., small strain shear modulus) using the bender element method technique. The small strain shear modulus (G_0) is used as a mechanical parameter to evaluate the shear stress transmission of the soil structure along with the erosion process. The comparison between erosion percentage and vertical strain change suggests the alteration in soil fabric after soil erosion. The G_0 monitoring results show that packings with a higher original fine particle content have a lower G_0 value, whereas the gap ratio and relative density present a positive relationship with G_0.

Keywords: suffusion; gap-graded soil; fine particle content; gap ratio; relative density

1. Introduction

Suffusion refers to the process in which fine particles migrate from the soil skeleton composed of coarse particles in the presence of seepage flow with the satisfaction of two conditions: one is that the critical hydraulic gradient, which initiates the outflow of eroded fine particles out of the soil specimen, is reached; the other is that the size of the constriction between coarse particles is large enough to allow fine particles to move. The internal stability of the soil structure against internal erosion is strictly correlated with the role of the fine particles within the soil. Fine particles that align weakly in voids between coarse particles tend to form unstable soil structures. Where the fine particles are placed as part of the soil skeleton and even separate the coarse-particle contacts, both coarse and fine particles participate in force chains, and the soil structure is believed to be internally stable against internal erosion. The metastable soil structure involves fine particles sitting within the soil skeleton while providing horizontal support to the soil. It is sensitive to vertical stress—the up-to-down seepage force. Suffusion is responsible for approximately half of the world's dam failures and seriously impacts the stability of water management buildings and the ecological environment.

One way to study the influence of fine particle content on suffusion would be to modify the initial fine particle content prior to erosion or to track the change in soil fabric and mechanical behavior with the loss of fine particles during erosion. These studies on mechanical performance with experimental work were less indicative of the understanding of the role of fine particles in soil mechanics [1]. The theory claimed that the fine particle content weakened the resistance to liquefaction when the relative density remained unchanged. For fine particle content, the value of 44% was thought to be the threshold value below which liquefaction resistance fell [2,3]. Mehdizadeh et al. [4,5] revealed that the initial content of fine particles impacted the mechanical behavior of gap-graded soils in a modified triaxial erosion device. A correlation between fine particle

content and fine particle erodibility was reported by Ke and Takahashi [6]. It confirmed the 37% fine particle content below which fine particles were unstable and migrated out of the soil skeleton under the influence of the seepage force. A similar statement was proposed by Chang and Zhang [7] that the stable soil fabric consisted of more than 35% fine particulate matter, below which an unstable soil structure would be formed. A rigid wall permeameter was adopted by Tian et al. [8] to study the impact of fine particulate matter content on internal erosion. In these works, it was found that increasing the fine particulate content would decrease the erosion risk and improve the mechanical performance of the solid fabric, especially when coarse particulate matter dominated the soil structure. However, few studies have focused on the real-time evaluation of suffusion in terms of volume and G_0 change, which would be detailed in this research with the assistance of the bender element technique.

The gap ratio (Gr) refers to the ratio between the maximum size of fine particles and the minimum size for coarse particles in a mixture packing. The stability criteria evaluation is applicable when the gap ratio is less than 3 [7]. Zhu et al. [9] evaluated erosion initiation conditions with a variety of particle size distributions, i.e., the gap ratio and coarse particle content. The authors stated that internal erosion would be initiated with a coarse particulate content in the range of 60% to 95% when the gap ratio was greater than 9.5. Alternative soil stability thresholds were proposed in an early stage in soil mechanics studies—a gap ratio of less than 4 or 5 was thought to promote a stable soil fabric within the soil structure of wide graded soils [10,11]. However, in addition to the erosion initiation criteria, little attention has been focused on the volume change post erosion in different initial gap ratios. This study would quantify the impact of gap ratio on soil fabric in terms of soil volume and post-erosion PSD in different sample sections.

Chen et al. [12] claimed that increasing the initial relative density (from 20% to 80%) would result in a higher drained failure strength based on a triaxial erosion apparatus with gap-graded soils. Chitravel et al. [1] suggested that the cyclic strength of samples after erosion was improved independent of the variation in the initial relative density (45% to 84%) with experimental work on broadly graded volcanic ash. An investigation concerning mechanical behavior asserted that relative density did not have an obvious impact on the relationship between the post-cyclic excess pore water pressure and the undrained shear stress [13]. Relative density, on the other hand, was confirmed to govern liquefaction resistance with a constant fine particle content [2]. Even less was known about the impact of relative density on the mechanical behavior of soil structure. To draw a comprehensive conclusion of the impact of relative density, this study investigates the reaction of a small-strain shear modulus with the wide variation in initial relative density (30%, 60%, and 90%).

Loss of soil particles due to detachment, degradation, or erosion would reduce the global volume of soil samples and impact the force transmission within the soil structure. This erosion process changes the particle size distribution and hence the overall volume that is correlated with the content of the particles [14]. Fam et al. [15] conducted erosion tests with gap-graded soils (i.e., the mixture of sand and salt) and investigated the relationship between the change in bulk volume and the small strain shear modulus using triaxial erosion devices. A reduction in shear strength was observed with only a slight change in volume during the erosion process. In the studies which adopted the oedometer to investigate the volume change (i.e., the settlement under oedometric conditions) of the soil specimen using salt–sand mixtures, settlement was directly assessed by the percent change in sample height. The result confirmed that the dissolution of the particles obviously had an impact on the change in soil volume while the packing was compared to the mass percentage of soluble salts [14–17].

Bender elements have been adopted for soil mechanics studies for long-term use since the first application by Shirley and Hampton [18]. Analytical and experimental studies regarding shear wave velocity monitoring have validated bender element techniques with installation on the erosion devices in an appropriate range of wave frequencies [19,20].

Eseller-Bayat et al. [21] studied both shear waves and compressional waves with a large liquefaction tank with the insertion of bender elements and bending discs at the rigid side walls, and the results confirmed that these shear-wave transducers were able to track shear waves and shear moduli at small strains with special designs to overcome electromagnetic interference. Montoya et al. [22] detailed the assembly of bender elements with the choice of cables, waterproofing materials, conductive coatings, etc., by considering the minimization of crosstalk and interferences from the rigid side wall. In addition, three types of bender element mounting approaches were proposed to achieve a satisfied coupling between soil and bender elements [22–26].

In this study, three layers of bender element pairs horizontally anchored on the side wall of the rigid wall permeameter are employed to investigate the impact of suffusion on shear wave transmission and hence G_0. The bender element system couples to the erosion system to monitor the real-time change in erosion percentage along with the corresponding mechanical behavior. This study also testifies the change in global volume of soils, as well as the post-erosion particle size distribution, suggesting the alteration in the soil fabric due to suffusion. As it enables the erosion process and real-time G_0 change to be tracked simultaneously, this study would contribute to the monitoring of water management buildings in terms of stability and damage risk.

2. Methodology

2.1. Apparatus

The acrylic cylinder used in this study allows for visualization of the erosion process and the change in global volume, with an outer diameter of 110 mm and a thickness of 10 mm (Figure 1). Three layers of holes are uniformly fabricated along the side wall of the chamber within the 33 mm gap, with an additional layer added for redundancy. Two additional holes are perpendicular to the bender elements for pressure transducer installation. Water leakage is reduced by Teflon carefully applied between the screws and the modular bender element. A fixed vertical loading of 27.56 kPa is provided on the top of sample through a loading bar.

In the erosion test system, a water tank is used to provide an infiltration flow from the top to bottom of the specimen with control of the flow velocity by a flow meter (Figure 2). De-aired water is supplied by a water pump to meet the hydraulic gradient criteria which is below one for internal erosion [27], and to initiate erosion in the specimens. Effluent from the bottom of the rigid wall permeameter discharges into the collection tank to allow for separation of the water from the deposited eroded fine particulate matter. Separated water is spilled into the water tank carrying few soil particles. The digital scale allows the extracted fine particles to be weighed and monitored in real-time, while the additional water drains into the water reservoir at the end of the system.

A bender element system couples with the erosion testing system to achieve the real-time tracking of shear wave velocity horizontally through the studied soils (Figure 3). This should give some new insights into the change in soil fabric caused by internal erosion. The transmission of shear wave signals is generated and amplified in advance of traveling through soil specimens. Hence, the received shear waves are restrengthened by a signal amplifier after the signal intensity is attenuated after travelling through specimens. Paired bender elements are placed face to face and extrude into the specimen. The bender element sheets are parallel with the flow direction to prevent damage. The oscilloscope plays a vital role in collecting, displaying, and comparing transmitting and receiving shear waves to infer travel time and hence shear wave speeds.
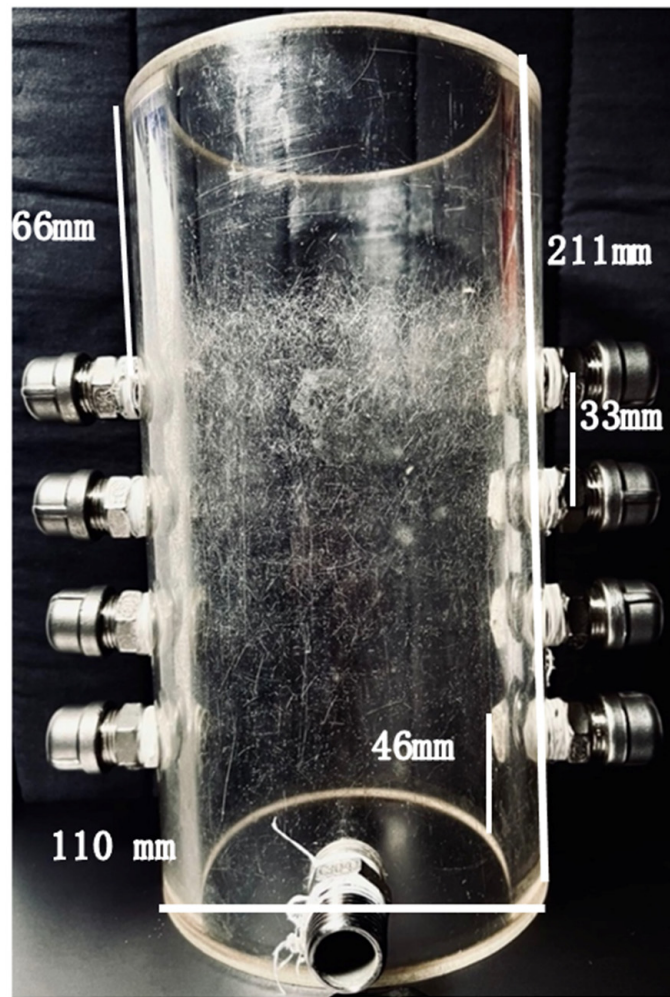
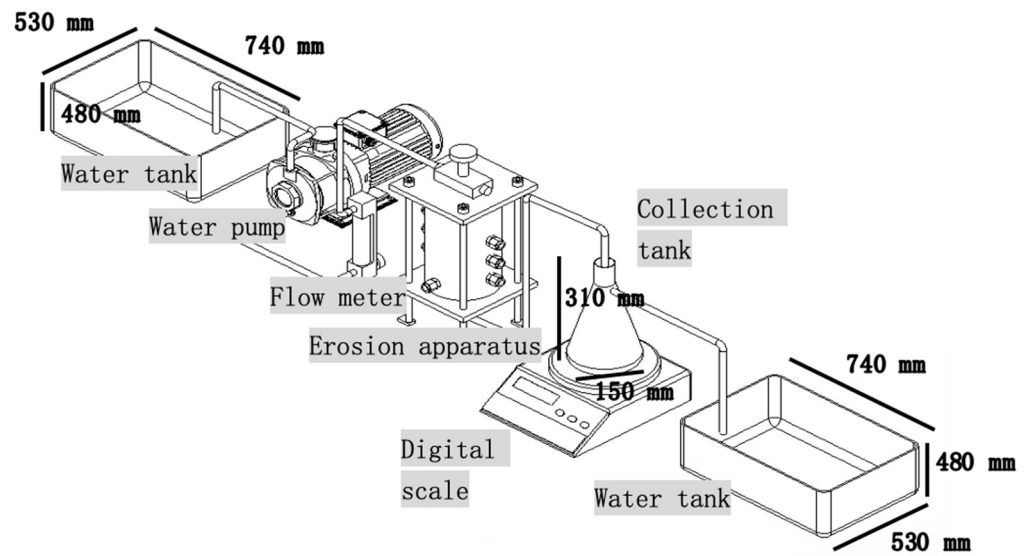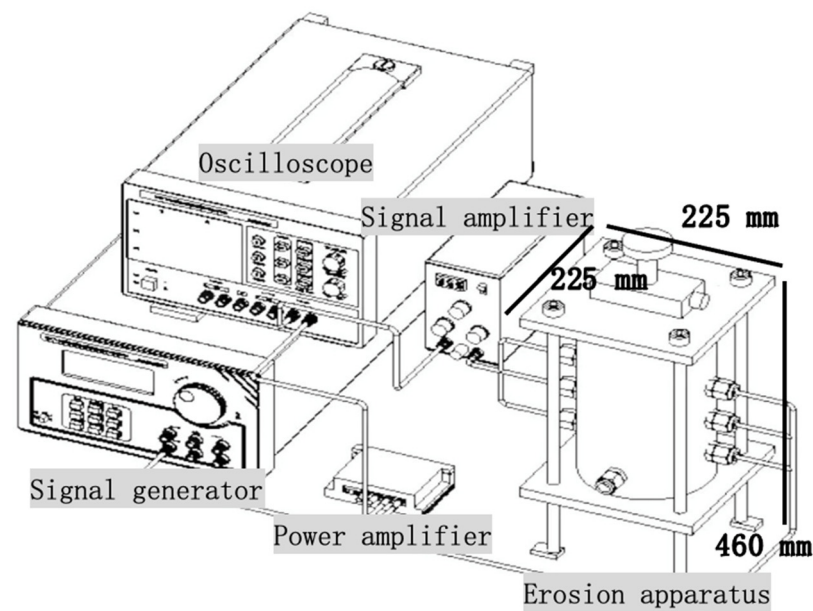**Figure 1.** Erosion chamber with holes along the side wall.

Figure 2. Overview of the erosion testing system.

Figure 3. Overview of the bender element system.

2.2. Bender Element Assembles

Careful fabrication and assembly of the modular bender element are crucial to achieve reliable shear waves (Figure 4). The modular bender element with careful design would alleviate rigid wall boundary effects, water leakage issues, and electromagnetic interference. In this study, the shielded twisted pair cable is soldered to bender elements using a parallel connection method with painting silver conductive adhesive paste, in which case the electromagnetic coupling effect is further reduced. To precisely anchor the bender element to the hollow screw with the injection of silica gel, a specially designed curing mold is adopted [21]. The silica gel and polyurethane coating on the bender element are believed to prevent interference of the water flow on the signal quality and address waterproofing problems. Screw tape with Teflon while coupling to the Plexiglass chamber is used to reduce the leakage of water to the sides. The grinding edges of the bender elements help to enhance the durability as soil particles migrate around the signal transducers during the erosion process.
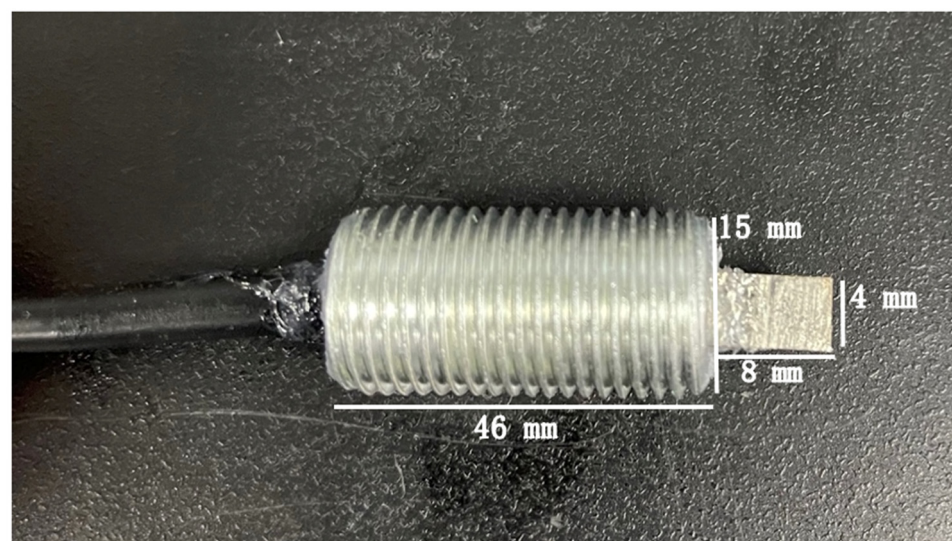
Figure 4. The modular bender element.

2.3. Specimen Preparation Technique

This study tests several mixtures of non-cohesive gap-graded quartz sand with varying fine particle contents and gap ratios. The fine particulate content varies between 15% and 35% with a 10% increase, and the gap ratio ranges from of 3.2 to 5.2 and 9.8, in which case the soil sample in either the steady state, unstable state, or metastable state is covered in the present study [10,11,28]. Table 1 summarizes the basic characteristics of mixture packings. The internal stability of the studied mixture packings is evaluated using available geometrical methods prior to erosion testing [7,10,11,29–31]. e_{min} and e_{max} are derived based on γ_{min} and γ_{max} by soil index density tests. Moist soil samples are prepared with an initial moisture content of 6% followed by placement in the chamber layer by layer. The modified moist tamping method is proposed to provide a relatively homogenous soil specimen that compensates for the effect of the weight of the top layers by adopting a variety of soil layers [32]. The percentage of undercompaction is varied to achieve the desired relative density in each layer. For the sample of 60% relative density, the bottom layer is 7% and the top layer is 0%. The weight and height of each layer are derived based on the total number of layers, the overall weight of the sample, and the overall height. Special care must be taken in specimen preparation and placement to avoid the destruction of extruding bender elements within the chamber.

Table 1. Fundamental geometrical properties of studied soils.

Gr	Fc	Rd	Soil Gradation					e_{max}	e_{min}
			D_{60} (mm)	D_{30} (mm)	D_{10} (mm)	C_u	C_c		
		30%	1.8	1.4	0.19	9.5	5.7	0.70	0.44
5.2	15	60%	1.8	1.4	0.19	9.5	5.7	0.70	0.44
		90%	1.8	1.4	0.19	9.5	5.7	0.70	0.44
3.2		60%	1.5	0.7	0.14	10.7	2.3	0.63	0.40
		30%	1.7	1.3	0.14	12.1	7.1	0.67	0.36
5.2	25	60%	1.7	1.3	0.14	12.1	7.1	0.67	0.36
		90%	1.7	1.3	0.14	12.1	7.1	0.67	0.36
9.8		60%	1.8	1.2	0.1	18.0	8.0	0.77	0.29
		30%	1.6	0.25	0.12	13.3	0.3	0.62	0.38
5.2	35	60%	1.6	0.25	0.12	13.3	0.3	0.62	0.38
		90%	1.6	0.25	0.12	13.3	0.3	0.62	0.38

2.4. Erosion Testing Regime

The erosion test regime is summarized in Table 2, with each specimen named in a way that shows the fine particle content (e.g., F15), gap ratio (e.g., G5.2), and relative density (e.g., R60). Above the specimen, a fixed vertical load is attached via a stainless-steel loading bar. The inlet flow rate is controlled around 600 mL/min with the test time around 120 min for each erosion test. Test trials have verified that the seepage flow rate allows the migration of loosely seated fine particles to be stimulated while maintaining soil integrity.

Details of the bender element operation regarding the setting of the operating frequency are given in Table 3. The mass density of soil and the shear wave velocity determine the small-strain shear modulus. The travel time of each sample is directly captured in real-time by the oscilloscope. With slight tuning, the frequency is tuned around 5 kHz to achieve the optimal shear wave forms and hence an accurate travel time with the peak-to-peak travel time method.

Table 2. Erosion test regime for soil fabric change evaluation.

Tested Soil	Loading	Erosion		Initial Water Content
Specimen	Vertical Pressure (kPa)	Inflow Velocity (mL/min)	Duration (min)	Percentage (%)
F15-G5.2-R60	27.56	600	120	6
F25-G5.2-R60	27.56	610	117	6
F35-G5.2-R60	27.56	600	122	6
F25-G3.2-R60	27.56	590	122	6
F25-G9.8-R60	27.56	605	119	6

Table 3. Shear wave transition monitoring of top layers.

Sample Code	Mass Density	Frequency	Travel Time	Shear Wave Velocity	G_0
	(kg/m³)	(kHz)	(µs)	(m/s)	(MPa)
F15-G5.2-R30	1.77	5.0	1250	70.40	8.76
F25-G5.2-R30	1.82	5.3	1410	62.41	7.52
F35-G5.2-R30	1.85	5.2	1490	59.06	6.47
F15-G5.2-R60	1.86	5.0	1230	71.54	9.51
F25-G5.2-R60	1.93	5.1	1300	67.69	8.84
F35-G5.2-R60	1.94	5.1	1350	65.19	8.26
F15-G5.2-R90	1.96	5.0	1190	73.95	10.70
F25-G5.2-R90	2.06	5.1	1280	68.75	9.73
F35-G5.2-R90	2.04	5.0	1310	67.18	9.22

3. Results and Discussion

This study monitors the erosion process by continuously tracking the weight of the eroded fine particles within the 2 h duration, which has been verified to complete the erosion testing by trial erosion tests (Figure 5). Suffusion tends to be more severe in the sample with higher initial fine particle contents. In the case of F35-G5.2-R60, the weight of eroded fine particles fluctuates around 80 g, which is three times more than that of F15-G5.2-R60. Regardless of the initial fine particle content, the test remains at a high erosion rate for the first 20 min after erosion initiation. This could be explained by the fact that F35-G5.2-R60 has higher potentially unstable fine particles that are susceptible to erosion. After the first plateau, F35-G5.2-R60 reaches a new peak at about 40 min and then drops to around 80 g, which could be attributed to the stronger jet flow with plenty of fine particles injected into the weighting device along with the effluent. It is confirmed that 120 min is sufficient to complete erosion as there is no obvious change in eroded particles detected after 60 min.

The particle size distribution before and after erosion is obtained for different layers of each soil to gain an understanding of the change in soil gradation due to erosion but also to better understand the movement of fine particles in the specimen as erosion takes place (Figure 6). With the increase in initial fine particle content, the gap between each original and post-erosion particle size distribution is more conspicuous, which suggests that the rate of fine particle erosion is much greater for those with more finer particles in the soil skeleton.
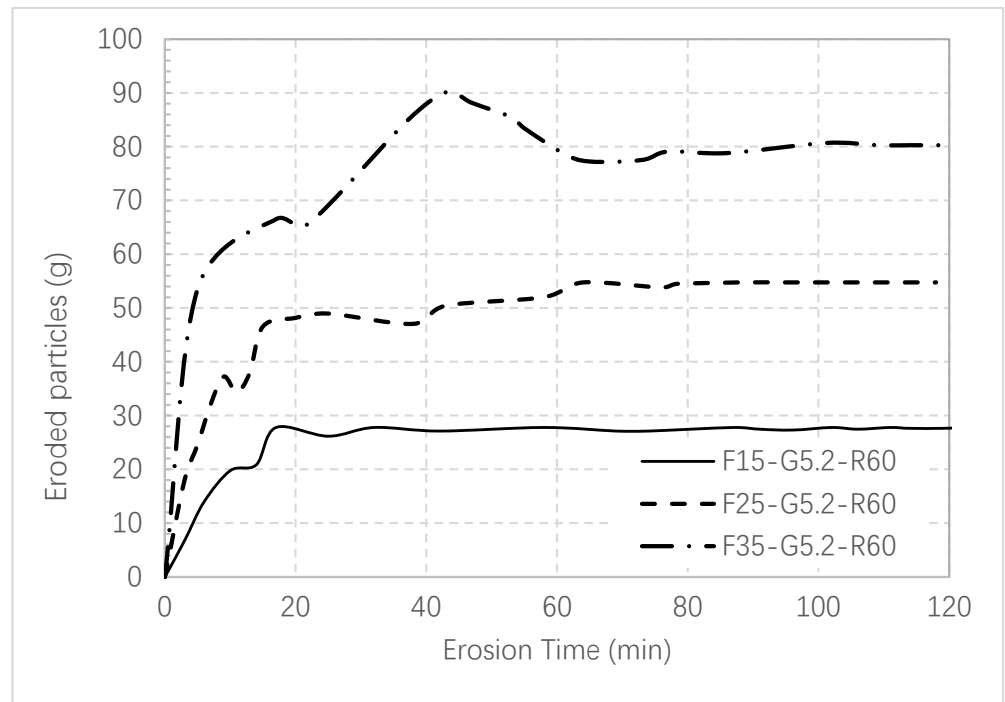
Figure 5. Erosion progress of studied mixture packings with variation in fine particle content.
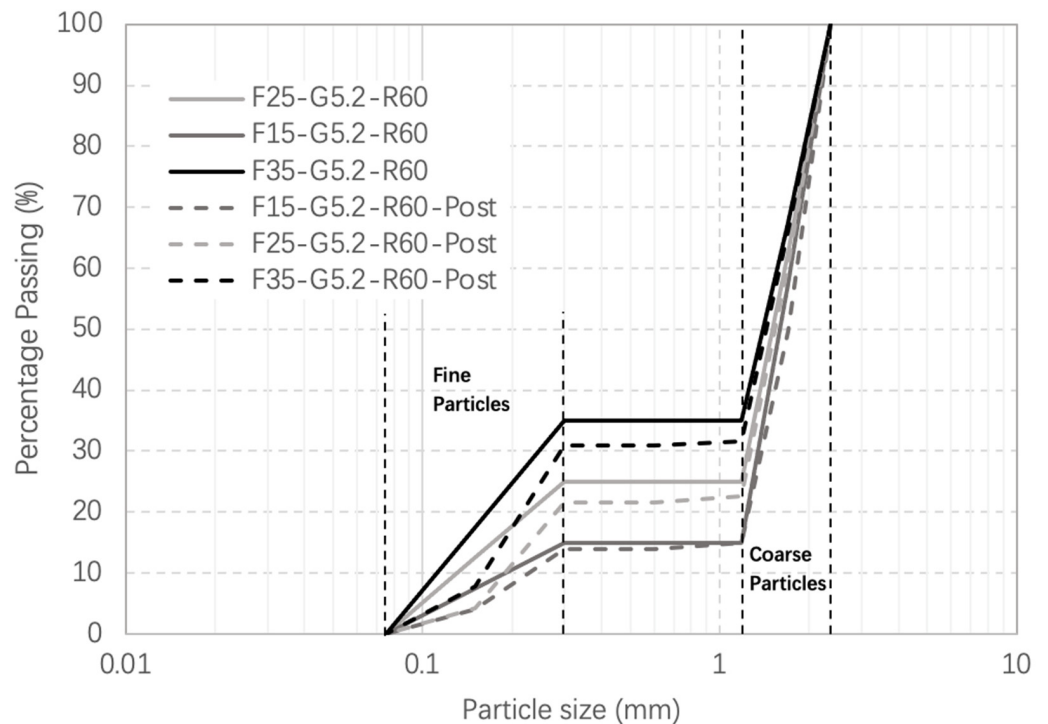

Figure 6. Particle size distribution of studied soils.

Erosion tests evaluate the settlement of soil specimens by measuring the height of the sample. The distance between the original and post-erosion sample height is identified, while the height change could refer to the volume change caused by erosion considering the rigid wall (Figure 7). The rate of volume change rises with increasing fine particle content. As the fines content increases from 25% to 35%, the volume increment increases from 3% to 4%, whereas the rate of change from 15% to 25% of the fines halves. Samples with a higher fines content are prone to settling since more severe particle migration could

occur in the inner soil layer. This could be explained by the reallocation of soil particles and their formation into a stable soil structure, during which the sample is further compressed. The trend of erosion percentage and global volume change is consistent. Particle migration and reallocation within the soil skeleton occurs, while the sample volume decreases at the same time as the loss of fine particles. It is worth mentioning that the increase in erosion percentage tends to slow down while the volume change rate accelerates. This potentially suggests that the impact from particle redistribution exceeds that of particle loss.
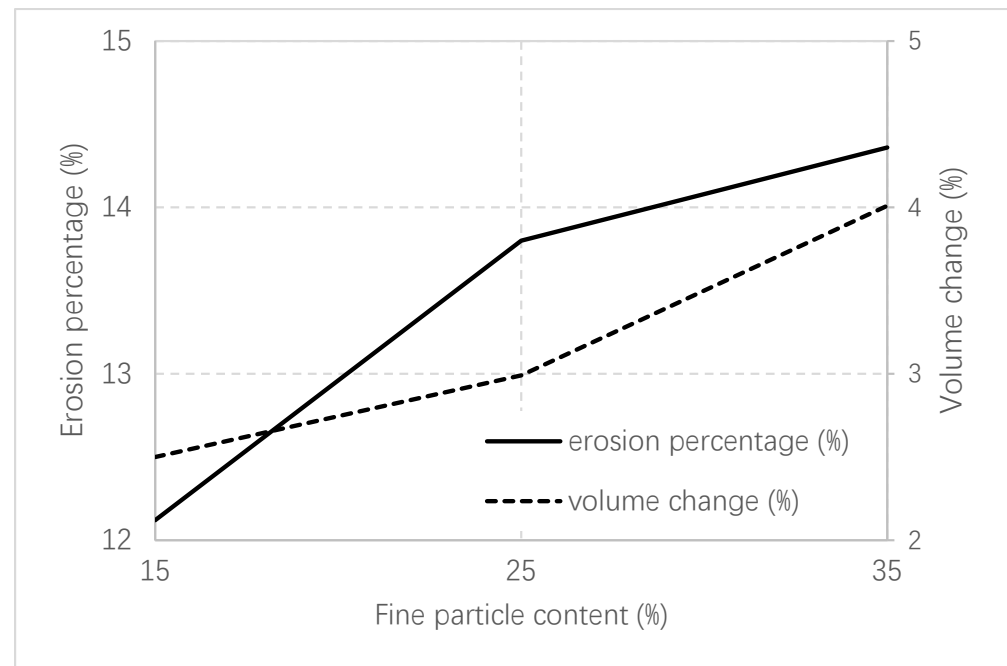

Figure 7. Comparison of erosion percentage and volume change.

Preferential paths are observed to appear at different locations of the rigid wall permeameter primarily during the early phase of erosion (Figure 8). An exceptionally higher level of loss of fine particles occurs at the top and bottom of the samples around the interface between the mesh and the sample (Figure 8a), where local settlement is observed with much loss of fine particles. The connecting location of either the pressure transducer or the bender element with the chamber also experiences distinct local deterioration (Figure 8b,e). In addition, apparent preferential erosional paths could be found at the cell periphery with a nonuniform distribution (Figure 8c,d), which might be attributed to the friction of the cell, although the center section of the specimen has been thoroughly impacted by the infiltration flow.

The impact of fine particle content and gap ratio on the overall volume change is presented in Figure 9. These tests confirm the positive relationship between the proportion of fine particles and the settlement of the sample. As the gap ratio increases, the packing of the soil tends to become less stable, which could be attributed to the less intense interior structure. A sample with a higher gap ratio, i.e., a less uniform particle size distribution, is subject to the more severe migration of fine particles, where interstices between coarse particles tend to be filled by finer granules; hence, there is a greater overall change in volume.

To investigate the mechanical performance of studied soils after the erosion process, the G_0 value is evaluated by three layers that align from the top to the middle and bottom of the sample (Figure 10). The small strain shear modulus of the bottom layer is distinctly higher than those of the top and middle layers, i.e., the bottom layer contains a higher number of fine particles. The increased particles are possibly caused by the migration of fine particles from the upper layers, and some of them become clogged in the bottom layer

before migrating into the collection tank. The high G_0 value of the top and middle layer indicates the decrease in fines content from the top sections of the sample. The G_0 value of the top layer is close to that of the middle layer, suggesting a similar regime of soil loss between the two layers.
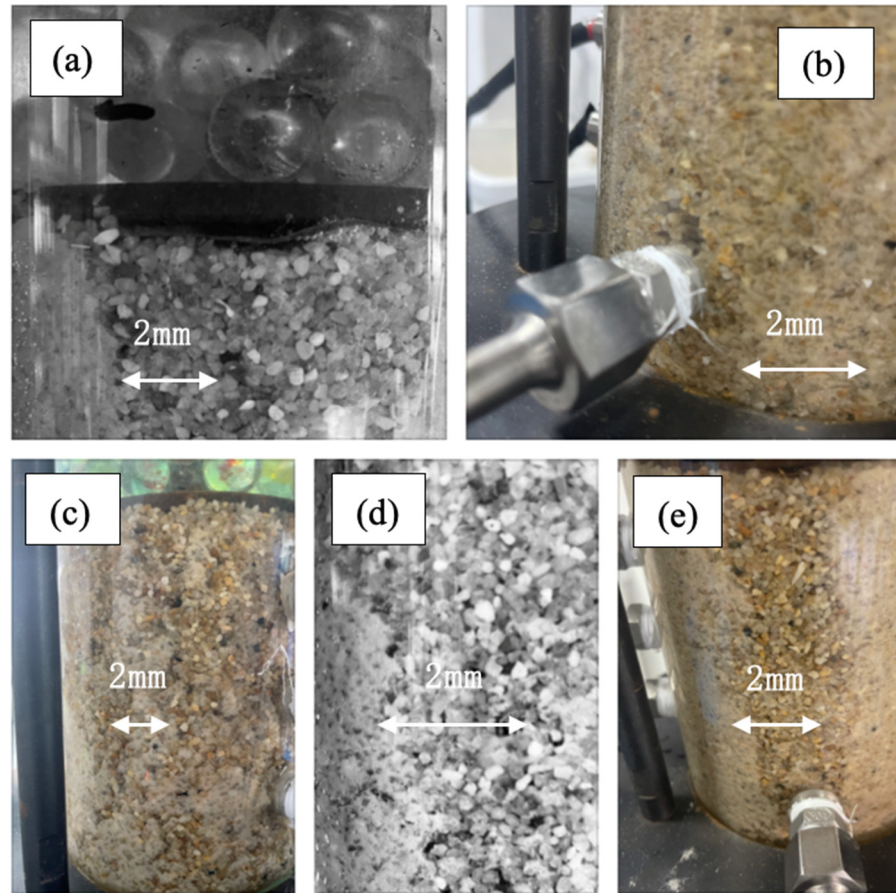
Figure 8. Preferential paths at different locations of the sample: (**a**) interface between mesh and sample; (**b**) interface between base plate and sample; (**c,d**) cell periphery; (**e**) interface between pressure transducer and sample.
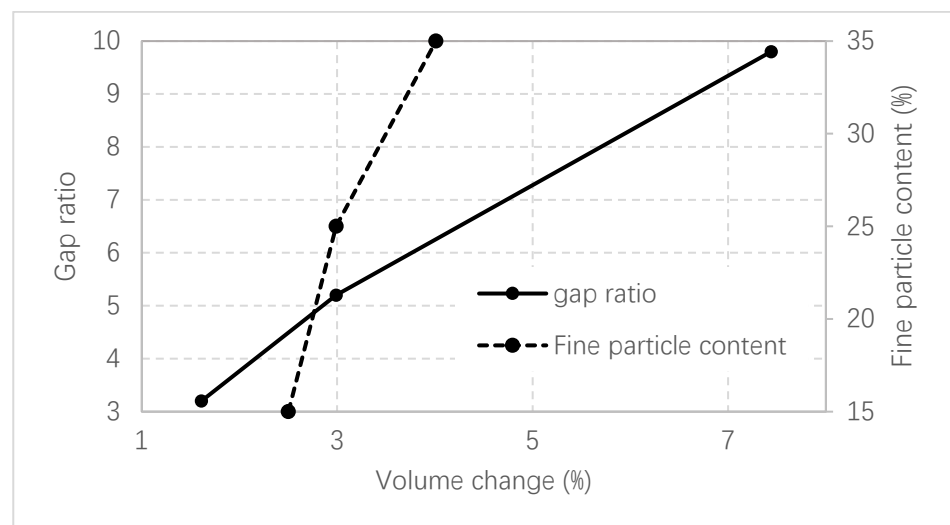

Figure 9. The diagram of volume change with the variation in gap ratio and fine particle content.
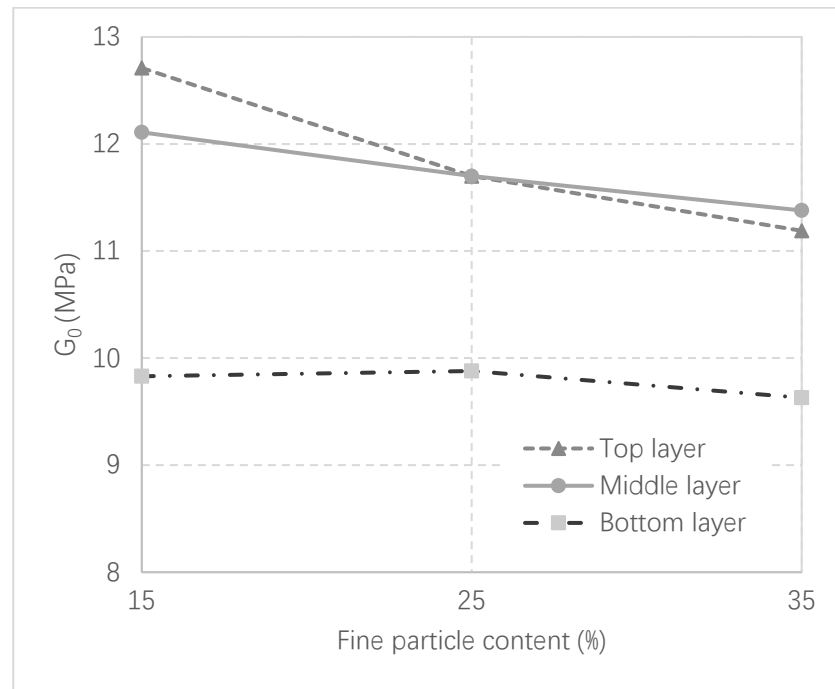
Figure 10. G_0 value in end time phase of three layers for studied soils.

The top layer, which directly suffers from the water flow, is selected as the representative to illustrate the impact of fine particle content and relative density in the initial phase of erosion. Figure 11 shows the evident positive correlation between relative density and G_0 value, whereas the fine particle content is opposite in magnitude to the small-strain shear modulus. A densified soil packing signifies an intensified soil structure with much intimate contact between soil granules.
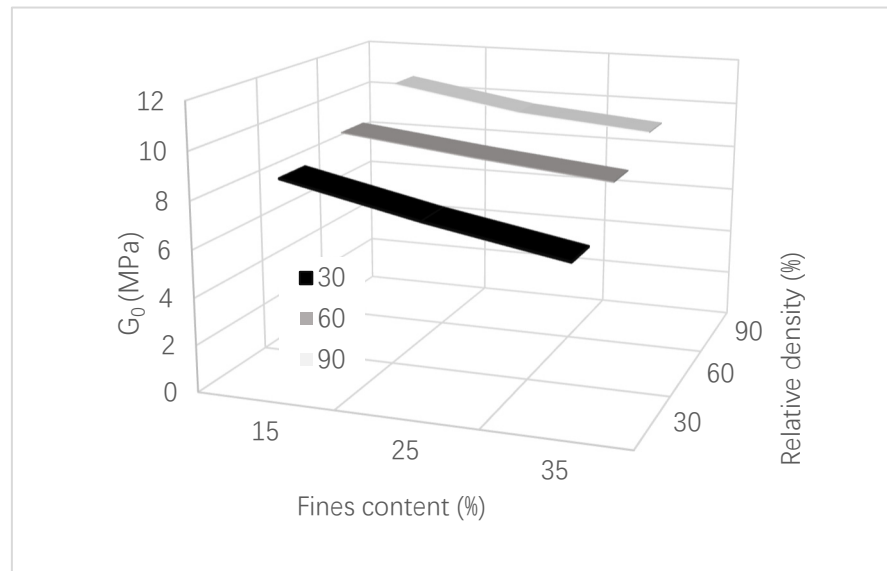
Figure 11. The diagram of the G_0 value varying with fines content and relative density in initial time phase for top layers.

4. Conclusions

This study adopted a self-regulating erosion apparatus and bender element system which enables the tracking of the erosion process and small-strain shear modulus in real-time by constantly weighing the eroded fine particles. This study investigates the impact

of the original fine particle content of gap-graded soils with varying gap ratio and soil compaction. Together with inspection of the bulk settlement of specimens and a comparison of pre- and post-erosion particle size distributions, the impact of suffusion on soil fabric alteration is explored. It is proposed that further research should focus on assessing local volume changes with the verification of numerical modeling. It is remarked that the main results of this study are as follows:

- The percent of erosion follows the trend of global volume change with increasing fine particle content in the 15% to 35% range. It is possible that the influence of particle readjustment could overwhelm fine particle loss. Either a higher initial fine particle content or gap ratio presents a severe change in global volume of the specimen.
- The soil particle content in the bottom layer obviously overshoots that of the upper soil layers by stacking, whereas the upper layers of the soil samples show a similar percentage and pattern of granule loss.
- Fine particle content has a negative impact on the transmission of shear waves through soil, whereas relative density is positively associated with shear wave velocity independent of the assumed unstable, metastable, and stable status of soils.
- Samples with a higher initial fine particle content are prone to experience more erosion percentage.
- The erosion process tends to take place concentrating on the initial 20 min despite varied fine particle proportions, with a slight fluctuation afterwards. For the sample with a higher fine particle content (35%), the effective erosion period is lengthened, but 120 min is sufficient to complete the erosion process with a reasonable surplus.

Author Contributions: C.D.: Conceptualization, Data Analysis, Investigation, Data Curation, Writing—Original Draft Preparation, Visualization. M.M.D.: Conceptualization, Methodology, Validation, Investigation, Supervision, Writing—Review And Editing. All authors have read and agreed to the published version of the manuscript.

Data Availability Statement: The data presented in this study are available on request from the corresponding author due to privacy.

Conflicts of Interest: The authors declare no conflict of interest.

References

1. Chitravel, S.; Otsubo, M.; Kuwano, R. Effects of internal erosion on the cyclic and post-cyclic mechanical behaviours of reconstituted volcanic ash. *Soils Found.* **2022**, *62*, 101111. [CrossRef]
2. Chien, L.-K.; Oh, Y.-N.; Chang, C.-H. Effects of fines content on liquefaction strength and dynamic settlement of reclaimed soil. *Can. Geotech. J.* **2002**, *39*, 254–265. [CrossRef]
3. Xenaki, V.C.; Athanasopoulos, G.A. Liquefaction resistance of sand–silt mixtures: An experimental investigation of the effect of fines. *Soil Dyn. Earthq. Eng.* **2003**, *23*, 1–12. [CrossRef]
4. Mehdizadeh, A.; Disfani, M.M.; Evans, R.; Arulrajah, A.; Ong, D.E.L. Mechanical consequences of suffusion on undrained behaviour of a gap-graded cohesionless soil-an experimental approach. *Geotech. Test. J.* **2017**, *40*, 1026–1042. [CrossRef]
5. Mehdizadeh, A.; Disfani, M.M.; Evans, R.; Arulrajah, A. Progressive in ternal erosion in a gap-graded internally unstable soil: Mechanical and geometrical effects. *Int. J. Geomech.* **2018**, *18*, 04017160. [CrossRef]
6. Ke, L.; Takahashi, A. Strength reduction of cohesionless soil due to in ternal erosion induced by one-dimensional upward seepage flow. *Soils Found.* **2012**, *52*, 698–711. [CrossRef]
7. Chang, D.S.; Zhang, L.M. Extended internal stability criteria for soils under seepage. *Soils Found.* **2013**, *53*, 569–583. [CrossRef]
8. Tian, D.; Xie, Q.; Fu, X.; Zhang, J. Experimental study on the effect of fine contents on internal erosion in natural soil deposits. *Bull. Eng. Geol. Environ.* **2020**, *79*, 4135–4150. [CrossRef]
9. Zhu, Q.; Su, L.; Liu, Z.; Wang, B. An evaluation method for internal erosion potential of gravelly soil based on particle size distribution. *J. Mt. Sci.* **2022**, *19*, 1203–1214. [CrossRef]
10. Kezdi, P.; Rosenbaum, M.B. Classification of ventricular extrasystoles according to form. *J. Electrocardiol.* **1969**, *2*, 289–297. [CrossRef]
11. Sherard, J.L. Sinkholes in dams of coarse, broadly graded soils. In Proceedings of the Transactions, 13th International Congress on Large Dams, New Delhi, India, 29 October–2 November 1979; Volume 2, pp. 25–35.

12. Chen, L.; He, J.; Yao, B.; Lei, C.; Zhang, Z. Influence of the Initial Relative Density on the Drained Strength Properties of Soils Subjected to Internal Erosion. *Soil Mech. Found. Eng.* **2019**, *56*, 273–279. [CrossRef]

13. Wang, S.; Luna, R.; Yang, J. Postcyclic behavior of low-plasticity silt with limited excess pore pressures. *Soil Dyn. Earthq. Eng.* **2013**, *54*, 39–46. [CrossRef]

14. McDougall, J.; Kelly, D.; Barreto, D. Particle loss and volume change on dissolution: Experimental results and analysis of particle size and amount effects. *Acta Geotech.* **2013**, *8*, 619–627. [CrossRef]

15. Fam, M.A.; Cascante, G.; Dusseault, M.B. Large and small strain proper ties of sands subjected to local void increase. *J. Geotech. Geoenviron. Eng.* **2002**, *128*, 1018–1025. [CrossRef]

16. Shin, H.; Santamarina, J.C. Mineral dissolution and the evolution of k 0. *J. Geotech. Geoenviron. Eng.* **2009**, *135*, 1141–1147. [CrossRef]

17. Truong, Q.H.; Eom, Y.H.; Lee, J.S. Stiffness characteristics of soluble mixtures. *Géotechnique* **2010**, *60*, 293–297. [CrossRef]

18. Shirley, D.J.; Hampton, L.D. Shear-wave measurements in laboratory sediments. *J. Acoust. Soc. Am.* **1978**, *63*, 607–613. [CrossRef]

19. Lee, J.-S.; Santamarina, J.C. Bender elements: Performance and signal interpretation. *J. Geotech. Geoenviron. Eng.* **2005**, *131*, 1063–1070. [CrossRef]

20. Salgado, R.; Bandini, P.; Karim, A. Shear strength and stiffness of silty sand. *J. Geotech. Geoenviron. Eng.* **2000**, *126*, 451–462. [CrossRef]

21. Eseller-Bayat, E.; Gokyer, S.; Yegian, M.; Deniz, R.; Alshawabkeh, A. Bender Elements and Bending Disks for Measurement of Shear and Compression Wave Velocities in Large Fully and Partially Saturated Sand Specimens. *Geotech. Test. J.* **2013**, *36*, 20120024. [CrossRef]

22. Montoya, B.M.; Gerhard, R.; DeJong, J.T.; Wilson, D.W.; Weil, M.H.; Martinez, B.C.; Pederson, L. Fabrication, operation, and health monitoring of bender elements for aggressive environments. *Geotech. Test. J.* **2012**, *35*, 728–742. [CrossRef]

23. Brandenberg, S.J.; Choi, S.; Kutter, B.L.; Wilson, D.W.; Santamarina, J.C. A bender element system for measuring shear wave velocities in centrifuge models. In Proceedings of the 6th International Conference on Physical Modeling in Geotechnics 2006, Hong Kong, China, 4–6 August 2006; pp. 165–170.

24. da Fonseca Ferreira, C.M.; da Fonseca, A.J.P.V. *International Parallel Tests on Bender Elements at the University of Porto, Portugal*; University of Porto: Porto, Portugal, 2005.

25. DeJong, J.T.; Fritzges, M.B.; Nüsslein, K. Microbially induced cementation to control sand response to undrained shear. *J. Geotech. Geoenviron. Eng.* **2006**, *132*, 1381–1392. [CrossRef]

26. Fu, L.; Zeng, X.; Figueroa, J.L. Shear wave velocity measurement in centrifuge using bender elements. *Int. J. Phys. Model. Geotech.* **2004**, *4*, 1–11. [CrossRef]

27. Terzaghi, K. *Erdbaumechanik*; Franz Deuticke: Vienna, Austria, 1925.

28. Shire, T.; O'Sullivan, C.; Hanley, K.J.; Fannin, R.J. Fabric and Effective Stress Distribution in Internally Unstable Soils. *J. Geotech. Geoenviron. Eng.* **2014**, *140*, 04014072. [CrossRef]

29. Dallo, Y.A.H.; Wang, Y.; Ahmed, O.Y. Assessment of the internal stability of granular soils against suffusion. *Eur. J. Environ. Civ. Eng.* **2013**, *17*, 219–230. [CrossRef]

30. Moraci, N.; Mandaglio, M.C.; Ielo, D. Analysis of the internal stability of granular soils using different methods. *Can. Geotech. J.* **2014**, *51*, 1063–1072. [CrossRef]

31. US. Army. *Filter Experiments and Design Criteria*; Technical Memorandum: Vickburg, MI, USA, 1953; Volume 52, pp. 3–360.

32. Ladd, R.S. Preparing test specimens using undercompaction. *Geotech. Test. J.* **1978**, *1*, 16–23. [CrossRef]